Acta Oceanol. Sin., 2022, Vol. 41, No. 9, P. 50–59
https://doi.org/10.1007/s13131-022-1989-1
http://www.aosocean.com
E-mail: ocean2@hyxb.org.cn

Temporal and spatial changes of the basal channel of the Getz Ice Shelf in Antarctica derived from multi-source data

Zemin Wang[1], Mingliang Liu[1], Baojun Zhang[1]*, Xiangyu Song[2, 3], Jiachun An[1]

[1] Chinese Antarctic Center of Surveying and Mapping, Wuhan University, Wuhan 430079, China

[2] School of Civil Engineering, Shijiazhuang Tiedao University, Shijiazhuang 050043, China

[3] Key Laboratory of Roads and Railway Engineering Safety Control (Shijiazhuang Tiedao University), Ministry of Education, Shijiazhuang 050043, China

Received 13 May 2021; accepted 3 December 2021

Abstract

Basal melting is an important factor affecting the stability of the ice shelf. The basal channel is formed from uneven melting, which also has an important impact on the stability of the ice shelf. Therefore, it has important scientific value to study the basal channel changes. This study combined datasets of Mosaics of Antarctica, Reference Elevation Model of Antarctica (REMA) and Operation IceBridge to study the temporal and spatial changes of basal channels at the Getz Ice Shelf in Antarctica. The relationships between the cross-sectional area and width of basal channel and those of its corresponding surface depression were statistically analyzed. Then, the changes of the basal channels of Getz Ice Shelf were derived from the ICESat observations and REMA digital elevation models (DEMs). After a detailed analysis of the factors affecting the basal channel changes, we found that the basal channels of Getz Ice Shelf were mainly concentrated in the eastern of the ice shelf, and most of them belonged to the ocean-sourced basal channel. From 2009 to 2016, the total length of the basal channel has increased by approximately 60 km. Affected by the warm Circumpolar Deep Water (CDW), significant changes in the basal channel occurred in the middle reaches of the Getz Ice Shelf. The change of the basal channels at the edge of the Getz Ice Shelf is significantly weaker than that in its middle and upper reaches. Especially in 2005–2012, the eastward wind on the ocean wind field and the westward wind around the continental shelf caused the invasion and upwelling of CDW. Meanwhile, the continuous warming of deep seawater also caused the deepening of the basal channel. During from 2012 to 2020, the fluctuations of the basal channels seem to be caused by the changes in temperature of CDW.

Key words: Getz Ice Shelf, basal channel, surface elevation, ICESat, DEM

Citation: Wang Zemin, Liu Mingliang, Zhang Baojun, Song Xiangyu, An Jiachun. 2022. Temporal and spatial changes of the basal channel of the Getz Ice Shelf in Antarctica derived from multi-source data. Acta Oceanologica Sinica, 41(9): 50–59, doi: 10.1007/s13131-022-1989-1

1 Introduction

The ice contained in the Antarctic ice sheet has the potential to raise the global sea level by more than 60 m (Fretwell et al., 2013). Ice shelf is the part of the ice sheet that extends over the ocean. It is very effective to slow down the rate of sea-level rise (Dupont and Alley, 2005; Fürst et al., 2016). Because of its direct contact with the atmosphere and ocean, ice shelf will be affected by many factors, and very sensitive to climate change (Joughin and Padman, 2003; Jenkins et al., 2010; Krabill et al., 2004; Rignot et al., 2013). Basal melting is the main way for Antarctica to lose ice and snow (Lazeroms et al., 2018; Pritchard et al., 2012), which has an important impact on the stability of the ice shelf (Jacobs et al., 2011; Joughin et al., 2010; Shepherd et al., 2010). Basal channels are formed and exists at the bottom of the ice shelf, similar to an inverted river (Wang et al., 2020). The basal channel was discovered in the floating part of Peterman Glacier and Songdo Glacier for the first time. After that, basal channels were found under most ice shelves in Antarctica (Rignot and Steffen, 2008; Stewart et al., 2004; Bindschadler et al., 2011; Payne et al., 2007). According to Alley et al. (2016), basal channels can be divided into three categories: (1) subglacially-sourced basal channel: basal channels originate from the ground line, and corresponds to the simulated subglacial river direction; (2) ocean-sourced basal channel: basal channels originate from the downstream position of the groundline, move in the direction of the ice stream, it may be curved, basal channels deepen to the edge of the ice shelf or ends in the ice lake; (3) grounding-line-sourced basal channel: basal channels have the characteristics of the first two basal channels, but it does not correspond to the simulated subglacial river.

Previous studies have shown that basal channels are more common at the bottom of the ice shelf where the basal melting is severe mainly related to the invasion of warm ocean water, such as the Circumpolar Deep Water (CDW) entering the channel at the bottom of the ice shelf (Fricker et al., 2009; Alley et al., 2016; Dow et al., 2018). The existence and change of the basal channel will affect the stability of the ice shelf. Alley et al. (2016) found that a large number of basal channels under the ice shelves would weaken the stability of the ice shelves along the coast of the Amundsen Sea. Moreover, Vaughan et al. (2012) and Sergien-

Foundation item: The National Natural Science Foundation of China under contract Nos 41941010 and 42006184; the Independent Scientific Research Project of the State Key Laboratory of Information Engineering in Surveying, Mapping and Remote Sensing.
*Corresponding author, E-mail: bjzhang@whu.edu.cn

ko (2013) simulated the internal stress of the ice shelf, thereby found that the basal channels would increase the internal stress of the ice shelf. Because the basal channels are distributed at the bottom of tens to hundreds of meters ice, only a small amount of ice-penetrating radar observations can directly and effectively depict them. However, due to the limited observed each year, the temporal and spatial changes of the basal channels are difficult to obtain from ice-penetrating radar data, even Operation IceBridge (OIB) observations. Therefore, the studies on the basal channel are mainly based on the surface remote sensing data over ice shelf. Satellite images have been used to map and study the distribution and its change of basal channels (Alley et al., 2016; Wang et al., 2020). However, this data can not be used to study the changes of depth and width of basal channel. Chartrand and Howat (2020) used the surface elevation observations from ICESat, ICESat-2, OIB and Reference Elevation Model of Antarctica (REMA) to document changes in the channel's shape and its lateral motion base on the assumption of hydrostatic equilibrium. Unfortunately, most of the ice shelves over areas of rapid basal channel are out of hydrostatic equilibrium (Chartrand and Howat, 2020). In other words, the results based on the hydrostatic equilibrium hypothesis may be inaccurate.

The Getz Ice Shelf, located in West Antarctica, whose length is more than 500 km and width is between 30–100 km, has experienced rapid basal melting (Rignot et al., 2013; Jacobs et al., 2013). And its basal melting rate has increased in recent years (Paolo et al., 2015). There is a bottom groove about 1 200 m deep between Duncan Peninsula and Wright Island in the east of the Getz Ice Shelf and the bottom of the Amundsen Sea. CDW enters the bottom of the Getz Ice Shelf through this deep groove to accelerate the basal melting of the Getz Ice Shelf (Paolo et al., 2015; Wei et al., 2020). Therefore, a detailed analysis of the temporal and spatial characteristics of basal channels has important scientific significance for the future analysis of the stability of the Getz Ice Shelf. This study combined Moderate Resolution Imaging Spectroradiometer (MODIS) images, REMA digital elevation models (DEMs), IceBridge radar data, ICESat-1 and ICESat-2 to study the temporal and spatial changes of the basal channel of the Getz Ice Shelf. Firstly, we identified the basal channels under the Getz Ice Shelf and studied their spatial distribution and its change. Then, we statistically analyzed and obtained the relationship between the basal channel shape (i.e., depth and width) and that of the corresponding surface depression. Thereby, the long-term changes in shape of the basal channels were obtained and studied. Finally, the factors affecting the change of basal channel were discussed.

2 Data

2.1 *MOA*

In this study, we used the image data from the MODIS Mosaics of Antarctica (MOA) imaging products co-produced by the National Snow and Ice Data Center and the University of New Hampshire (Scambos et al., 2007) to identify the spatial distribution of basal channels under the Getz Ice Shelf in 2009. The source images are collected by MODIS instruments on National Aeronautics and Space Administration (NASA) EOS Aqua and Terra satellites (Li et al., 2018). The spatial resolution of the images is 125 m. The image can completely cover the entire Antarctic region, through the removal of covered clouds, can clearly distinguish the surface features on the Getz Ice Shelf.

2.2 *REMA DEMs*

REMA DEMs are constructed from hundreds of thousands of stereo DEMs from tens of thousands of scene pairs of satellite imagery from WorldView-1, WorldView-2, WorldView-3, and Geoye-1 data by the Polar Geospatial Center (PGC) of the University of Minnesota (Howat et al., 2019). PGC provides DEMs product with spatial resolutions from 2 m, 8 m, 100 m, 200 m to 1 000 m (Noh and Howat, 2017). They can be freely downloaded from https://www.pgc.umn.edu/data/rema/. In this study, we use REMA DEMs to infer the shape of the basal channel and construct the time series of basal channels under the Getz Ice Shelf based on the relationship between the basal channel shape and that of the corresponding surface depression.

2.3 *OIB*

Since its implementation in 2009, the OIB have recorded a large amount observational data for the study of changes in sea ice, ice sheets, and ice shelves (Kwok and Kacimi, 2018). Its Radar Sounder payload, the Multichannel Coherent Radar Depth Sounder (MCoRDS), can provide ice shelf surface and bottom terrain with an along-track resolution of 25 m (Kurtz and Farrell, 2011; Farrell et al., 2011). In this study, we use these data (IRMCR2, version 1) to validate and screen the basal channel extraction results from MOA images and REMA DEM. According to Alley et al. (2016), Wang et al. (2020), and Chartrand and Howat (2020), the OIB data can directly and effectively identify basal channel under ice shelf. There were 6 tracks of OIB observations over the Getz Ice Shelf, shown in Fig. 1. We used them to observe the surface and bottom characteristics of the Getz Ice Shelf, and

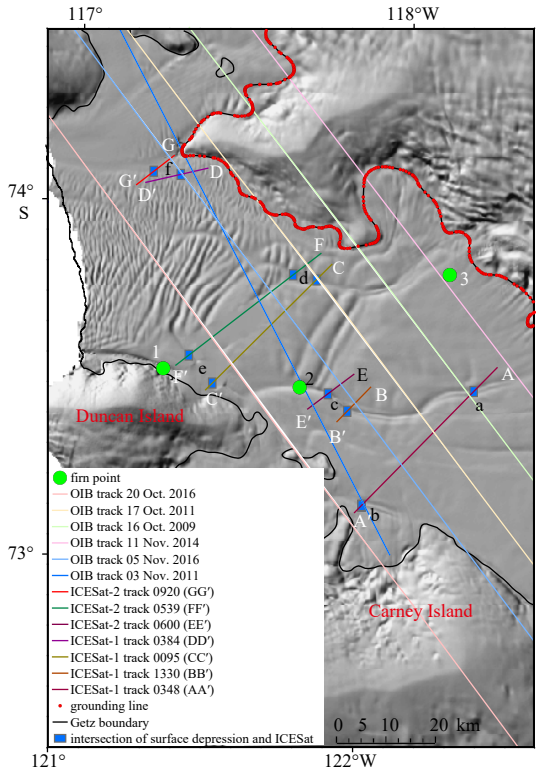

Fig. 1. Outline map of the eastern part of the Getz Ice Shelf. The background image is a REMA hillshade map. The blue rectangle indicates the intersection of the ICESat orbit and the recessed surface of the ice shelf. The colored thin lines indicate NASA OIB trajectories. The colored thick lines indicate the trajectories of ICESat-1 and ICESat-2, mark with white letters. The location of the analysis point is marked with black letters. The green point is location of surface elevation change due to surface process from the Institute for Marine and Atmospheric Research Utrecht Firn Densification Model (Ligtenberg et al., 2011, 2014).

identify the basal channels.

2.4 *ICESat-1 and ICESat-2*

ICESat-1 laser altimetry satellite was launched by the NASA on January 13, 2003 and stopped data collection on October 11, 2009. The new-generation ICESat-2 satellite resumed its acquisition mission in 2018 (Liu et al., 2020). The scientific purpose of them is to measure the height of the polar ice sheets and sea ice changes, cloud and aerosol height, and terrain and vegetation characteristic parameters (Hu et al., 2017; Borsa et al., 2014; Fricker and Padman, 2006). The lidar altimetry system carried by ICESat-1 and ICESat-2 have collected a large number of accurate surface elevation observations. This study used ICESat-1 (GLAH12, version 34) and ICESat-2 (ATL06, version 4) surface elevation observations to construct the time series of basal channels under the Getz Ice Shelf combined with REMA DEMs. Saturation corrections, Gaussian-centroid corrections, and inter-campaign Bias Corrections are applied to ICESat-1 measurements. The available ground trajectories distribution of ICESat-1 and ICESat-2 are shown in Fig. 1.

3 Identify basal channel of Getz Ice Shelf

According to previous studies (Alley et al., 2016; Wang et al., 2020; Chartrand and Howat, 2020), basal channels can be captured by the surface depression over ice shelf from remote sensing optical images, DEMs, and altimetry elevations identified by ice-penetrating radar. Here, we mapped and documented spatial distribution of basal channels on Getz ice shelves in 2009 and 2016 using MOA images and REMA DEM combined with OIB MCoRDS observations. In this study, basal channels were identified in three steps: (1) identifying the recessed area on the surface of the ice shelf utilizing the gray value of the optical remote sensing images; (2) verifying the depression area using DEMs and lidar altimetry data from ICESat-1 and ICESat-2; (3) validating and screening the basal channels using lower surface morphology of the ice shelf from OIB MCoRDS measurements. Figure 2c shows an example to validate the basal channels using OIB MCoRDS measurements.

The distribution of basal channels on Getz ice shelves in 2009 and 2016 are shown in Figs 2a and b, respectively. It can be clearly seen that basal channels of the Getz Ice Shelf are mainly

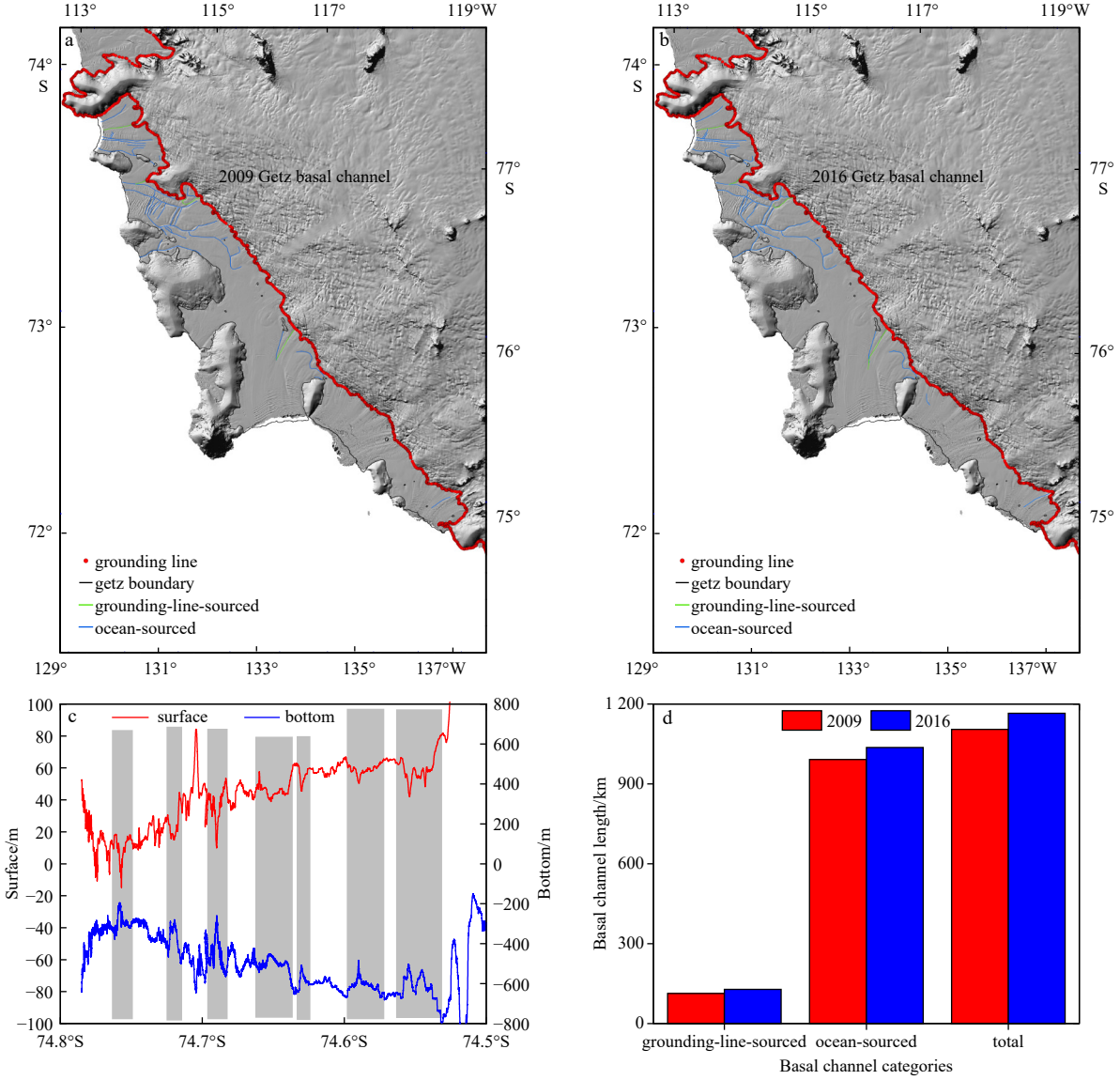

Fig. 2. Distribution of basal channels of the Getz Ice Shelf in 2009 (a) and 2016 (b); c. basal channels discrimination using OIB MCoRDS measurements; the gray marked part is the corresponding position of the basal channel; d. statistics of basal channels length.

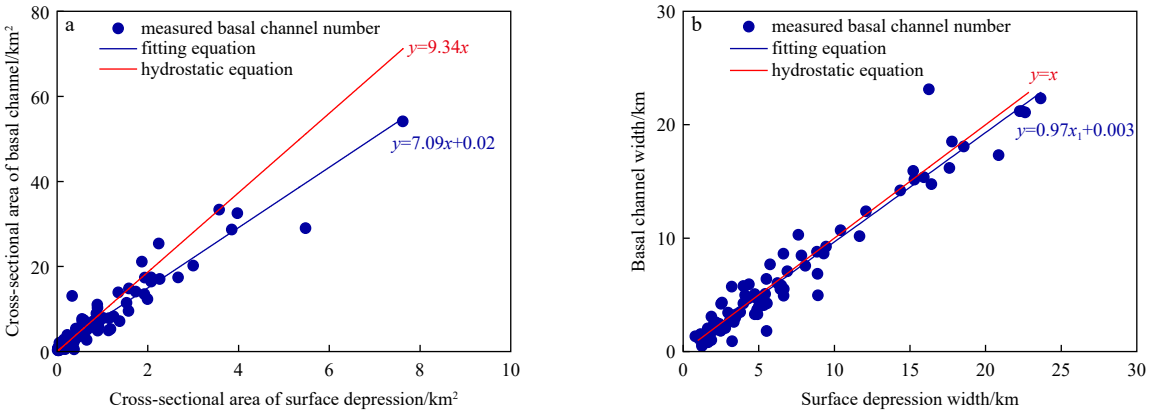

Fig. 3. The geometric relationship between the basal channels and the surface depression. a. Comparison of the cross-sectional area of the IceBridge trajectories across basal channels and those of the corresponding surface depression; the blue line is the linear fit as described by the linear relationship for the corresponding regression equation; the red line is their relationship when they are in hydrodynamic equilibrium; b. comparison of the cross-sectional width of the IceBridge trajectories across basal channels and those of the corresponding surface depression; the blue line is the linear fit as described by the linear relationship for the corresponding regression equation; the red line is their relationship when they are in hydrodynamic equilibrium.

distributed in the eastern part of the ice shelf. There are only grounding-line-sourced and ocean-sourced basal channels, not subglacially-sourced basal channel. And the number of ocean-sourced basal channel is significantly more than grounding-line-sourced basal channel. According to the detailed position of basal channels, we calculated the length of each type of basal channels in 2009 and 2016, as shown in Fig. 2d. The length of grounding-line-sourced basal channel was about 110 km in 2009, and the length of ocean-sourced basal channel is about 990 km. By 2016, they increased to 130 km and 1 030 km respectively. From 2009 to 2016, grounding-line-sourced basal channel has increased by about 20 km, ocean-sourced basal channel has increased by about 40 km, the total length of the basal channels has increased by about 60 km.

4 Relationship fitting

In addition to the confirmation of the basal channel, OIB data can also obtain the morphology of the ice shelf basal channel and its corresponding surface depression at the same time. We calculated the cross-sectional area and width of the IceBridge trajectory across basal channels of the ice shelf and those of the corresponding surface depression. The cross-sectional area of basal channels and the cross-sectional area of the corresponding surface depression is calculated by calculus. Then, we found that the cross-sectional area and width of basal channels and those of their corresponding surface depression are linear correlation, as shown in Fig. 3. Their relationship is obtained by linear fitting as follows:

$$y = 7.09x + 0.02, \tag{1}$$

where y is the cross-sectional area of basal channels, x is the cross-sectional area of the recessed surface corresponding to basal channels, the unit is km^2.

$$y_1 = 0.97x_1 + 0.003, \tag{2}$$

where y_1 is basal channels width, x_1 is the corresponding surface depression width for basal channels, the unit is km.

As shown in Fig. 3, the current basal channels did not reach hydrostatic equilibrium. Therefore, we should not use the hydrostatic equilibrium formula to infer basal channels changes from surface elevations. The width of basal channels and that of the corresponding surface depression is approximately equal. It implies that the relationship between the cross-sectional area of basal channels and the corresponding surface depression applies equally to the depth of basal channels and that of the corresponding surface depression. The depth of surface depression is more than that derived from hydrostatic equilibrium hypothesis, which may be caused by the influence of ice shelf surface process. Figure 4 shows the surface elevation change due to surface process. Therefore, we can use those linear relationships to invert the basal channel change from the surface depression change.

5 Long time series of basal channel

To study the long-term temporal and spatial variation characteristics of ice shelf basal channels, we need to construct the long time series basal channels by combining ICESat-1, ICESat-2, and REMA DEMs. Observed trajectories of ICESat-1 and ICESat-2 intersect with the basal channels in six regions, as shown in Fig. 1 marked a–f. Figure 5 shows the identification of the basal chan-

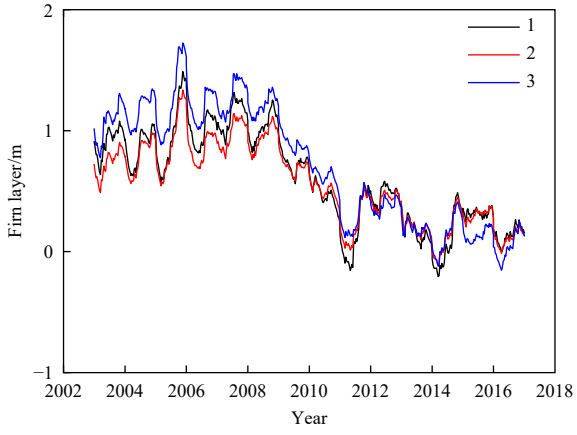

Fig. 4. Surface firn layer compaction thickness. The legend number corresponds to the number position of firn point in Fig. 1.

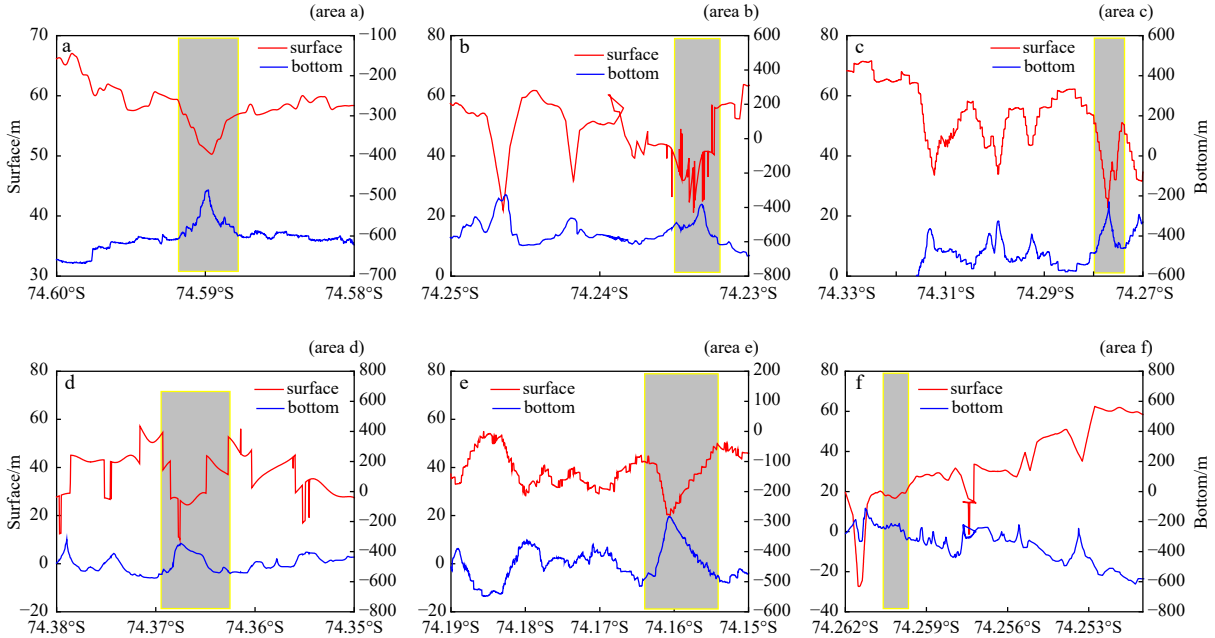

Fig. 5. Schematic diagram of determining the basal channel position through IceBridge data, corresponding to the position of the black letter mark in Fig. 1.

nels near those position with OIB data.

In these six intersection areas, we first developed long time series of surface depression by combining ICESat-1, ICESat-2, and REMA DEMs. The ice velocity of the Getz Ice Shelf is about 300 m/a (Mouginot et al., 2017). Therefore, when developing long time series, we need to normalize all the surface elevation data used in the calculation to unify them. The elevation peak or valley value of elevation of surface depression was selected to match each, because the peak or valley has obvious characteristics and is easy to match. In addition, we also moved their lowest points of the surface depression to the same vertical position to eliminate the northwest migration (Chartrand and Howat, 2020) of the basal channel caused by the motion of the ice shelf. The long time series of surface depression is shown in Fig. 6.

As mentioned in Section 3, there exists a linear relationship between the depth (or width) of basal channels of the Getz Ice Shelf and that of the corresponding surface depression. Therefore, the long time series of basal channels can be derived from the long time series surface depression. The time series of basal channels at six areas shown in Fig. 1 are shown in Fig. 7. It can be seen that the depth of basal channels at areas a–c has continued deepening from 2003 to 2012, but the depth of basal channels at

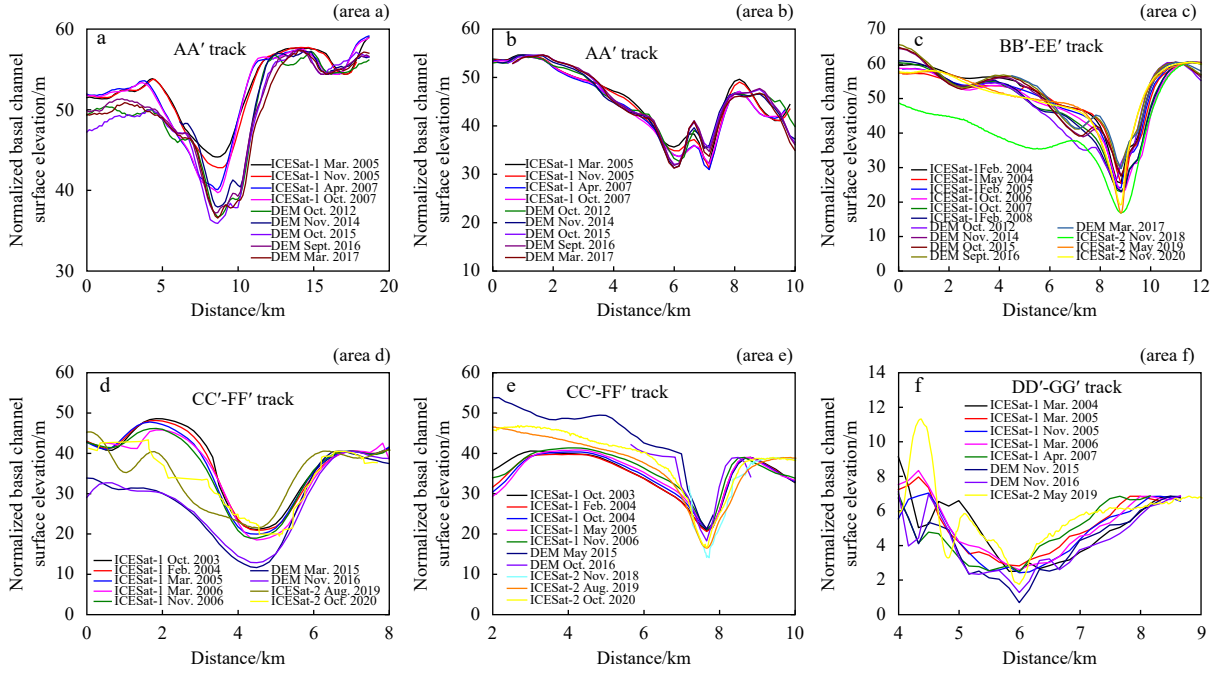

Fig. 6. The elevation time series of the surface depression at transects areas of a–f (a–f, respectively) shown in Fig. 1 by combining ICESat-1, ICESat-2, and REMA DEMs.

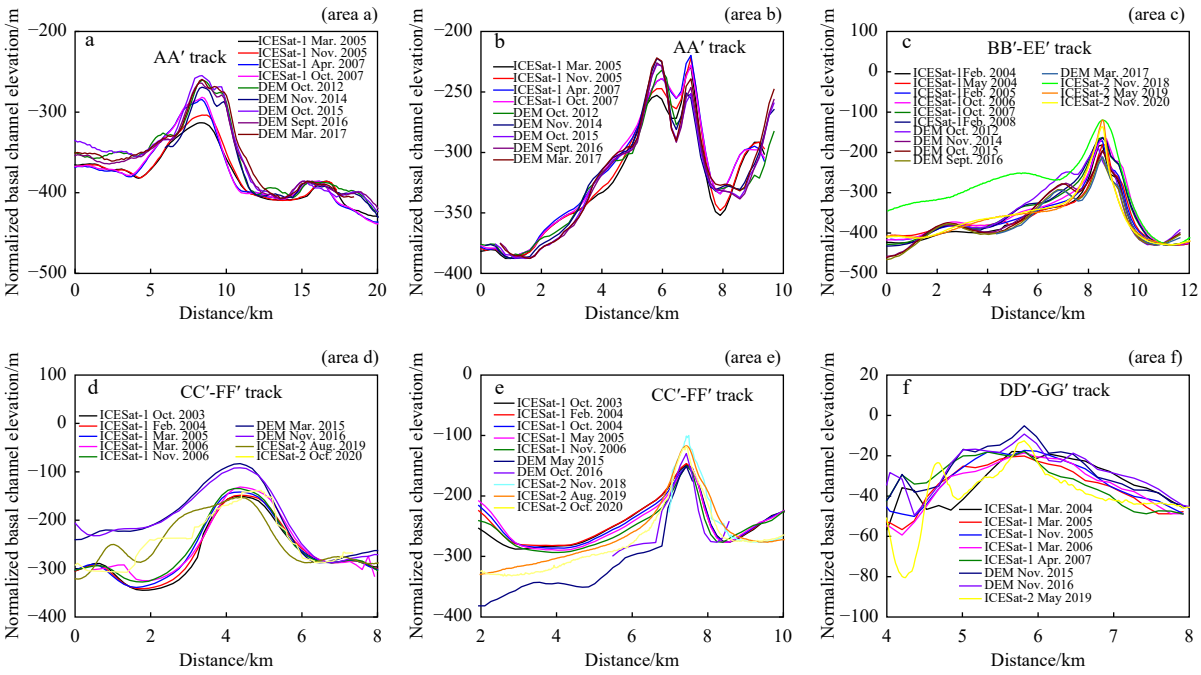

Fig. 7. The long time series of the basal channels at transects areas of a–f shown in Fig. 1 by combining ICESat-1, ICESat-2, and REMA DEMs.

areas d–f has turned shallow from 2019 to 2020. The basal channel at area a was deepened by 53.7 m from 2003 to 2017 with a mean rate of around 4.5 m/a. The basal channel at area b was deepened by 49.9 m from 2003 to 2017 with a mean rate of around 4.2 m/a. The basal channel at area c was deepened by 61.8 m from 2003 to 2017 with a rate of around 4.1 m/a. The basal channel at area d decreased to a minimum in 2015, which deepened by 66.9 m from 2003 to 2015 with a mean rate of about 5.6 m/a. The basal channel at area e was deepened by 29.7 m from 2003 to 2020 with a mean rate of around 1.7 m/a. The basal channel at area f decreased to a minimum in 2015, which deepened by 15 m from 2004 to 2015 with a mean rate of about 1.4 m/a. Taken together all the basal channel changes for a long time series, we can see that the basal channel at areas a–c were more significant with a rate of about 4.1–4.5 m/a. The basal channel at area d was the most significant with a rate around 5.6 m/a. The basal channel at areas e–f were the least obvious with a rate of about 1.4–1.7 m/a.

To analyze the variation of the basal channels of Getz Ice Shelf, we give the sea surface temperature (shown in Fig. 8), wind field (shown in Fig. 9), and deep seawater temperature (shown in Fig. 10). The sea surface temperature corresponding to the front of the Getz Ice Shelf is obtained by the Hadley Centre of the British Meteorological Service (Le Brocq et al., 2009). The wind field comes from the 10-m wind value of the European Center for Medium-Term Weather Forecast (Dee et al., 2011). The deep seawater temperature is from Jacobs et al. (2013) and Marine Geoscience Data System. As shown in Fig. 8, the surface temperature of seawater at the front of the Getz Ice Shelf has fluctuated several times and reached its lowest temperature in 2012. It can be seen from Fig. 9 that the wind direction and wind speed of the wind field near the Getz Ice Shelf in some periods during from 2003–2020 have changed representatively, and those changes could change basal melting of the ice shelf through impacting on the CDW (Holland et al., 2010; Padman et al., 2012; Dutrieux et al., 2014). The temperature of deep seawater at the front of the Getz Ice Shelf also has changed during the periods of 2000–2017, rising first and then falling.

6 Discussion

Basal melting of the Getz Ice Shelf is significantly affected by the nearby warm CDW (Arneborg et al., 2012; Jacobs et al., 1992; Silvano et al., 2018). There is a through about 1 200 m deep between Wright Island and Duncan Island in the east of the Getz Ice Shelf, which facilitates the unobstructed invasion of the CDW into the bottom of the Getz Ice Shelf (Wei et al., 2020; Assmann et al., 2019; Cochran et al., 2020). The stream axis of the Antarctic Circumpolar Current in the eastern of the Pacific sector is most southward, which more conducive to the upwelling of CDW to the continental shelf (Shi, 2018). Wei et al. (2020) discovered that basal melting of east of Getz Ice Shelf is concentrated along the

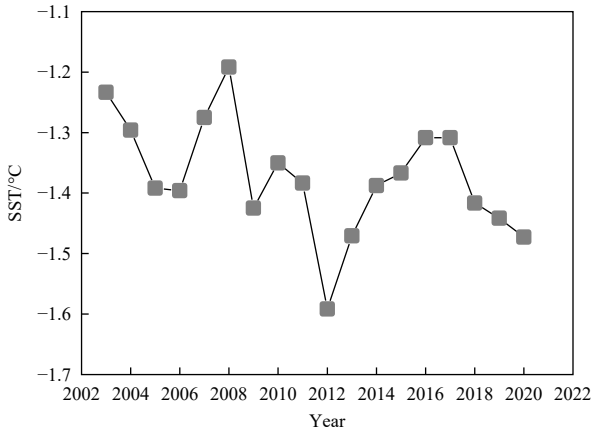

Fig. 8. The mean surface seawater temperature (SST) in different years from 2003 to 2020 at the eastern frontier of the Getz Ice Shelf.

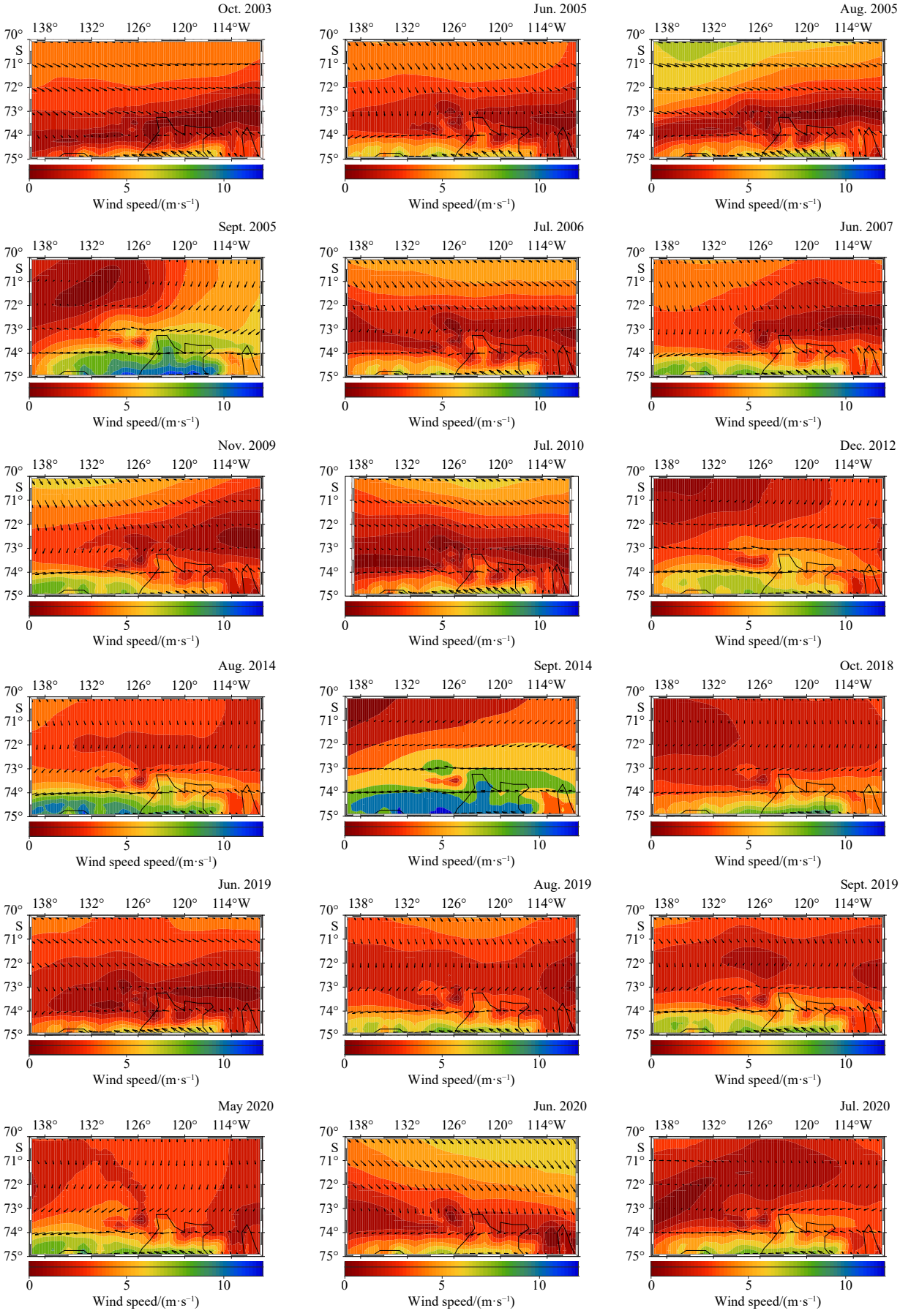

Fig. 9. Representative wind field data of some months from 2003 to 2020 of near the east of the Getz Ice Shelf.

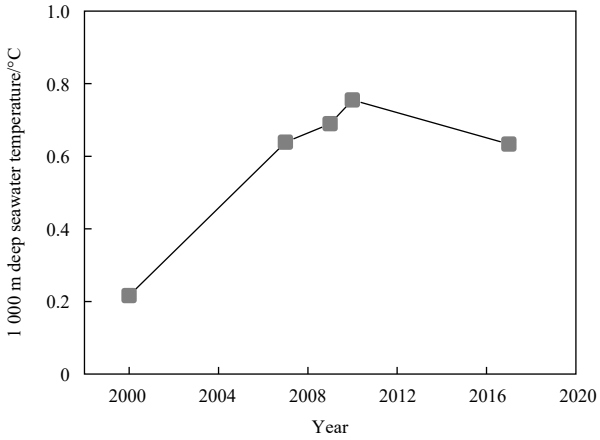

Fig. 10. Seawater temperature at depth of 1 000 m at the eastern tip of the Getz Ice Shelf.

grounding line especially where it intersects deep troughs and where the bottom of the ice shelf is below the 500 m thermocline depth over the troughs. They likely result from the warm CDW (Jacobs et al., 2013; Wei et al., 2020). From the ground line to the front of the ice shelf, basal melting rate is gradually weakened by the influence of CDW, and the basal melting rate of the ice shelf edge is least affected by CDW. Due to the greater influence of the CDW on basal melting, a large number of basal channels are formed under the east of the Getz Ice Shelf, and 90% of basal channels are ocean-sourced basal channel. Similarly, the melting at the basal channels above the trough in the middle and upper reaches is also more intense than that of basal channels at downstream of the ice shelf. It is consistent with the findings of this study that the deepening of the basal channel at areas a–d is significantly greater than that at e–f (see Fig. 7). It implies that the time-varying CDW intrusion has different effects on the changes of different basal channels.

The wind is an important factor in regulating the volume of Amundsen Sea CDW entering the continental shelf (Holland et al., 2010; Dinniman et al., 2012; Padman et al., 2012; Thoma et al., 2008; Steig et al., 2012; Dutrieux et al., 2014). The eastward wind energy on the surface of the Amundsen Sea drives the enhancement of the submarine undercurrent. The enhanced undercurrent further increases the transport of the extremely deep seawater volume between the Amundsen Sea and the Getz Ice Shelf and changes the depth of the isodensity line on the continental shelf through the Ekman pumping operation to enhance the heat content of the local CDW at the bottom of the Getz Ice Shelf (Dotto et al., 2019). The offshore wind on the surface of the continental shelf drives the surface seawater southward, causing the CDW at the bottom of the ice shelf to rise, increasing the basal melting rate of the ice shelf (Greene et al., 2017). It can be seen from Fig. 9 that there are several months every year, which promotes CDW invasion and upwelling to the bottom of the Getz Ice Shelf or increases the heat content of CDW, thereby accelerating the basal melting and deepening the basal channels.

Deep-sea temperature is also an important factor affecting basal melting of the ice shelf. Some studies have shown that basal melting rate of the ice shelf is positively correlated with the temperature of the deep seawater (Jenkins, 1999; Jenkins and Jacobs, 2008; Jacobs et al., 2011). From Jacobs et al. (2013) and Fig. 10, it can be seen that the temperature of deep seawater has continued to increase from 2000 to 2012 under the action of the wind field. As a result, the bottom channels at areas a–c have continued deepening during from 2003 to 2012.

As the temperature increases, warm surface seawater can also enhance basal melting rate of the ice shelf (Wang et al., 2020; Jacobs et al., 1992; Silvano et al., 2016). As shown in Fig. 8, the temperature of surface seawater near the front of the east of the Getz Ice Shelf fluctuated many times from 2003 to 2020. However, we did not find any relevant changes in the basal channels of the ice shelf. It may be because the Getz Ice Shelf is so thick that the temperature change of the surface seawater can not affect the basal melting of the ice shelf. The observed surface seawater temperature only represents the temperature of surface seawater at a depth of 1–20 m. Even if the heat exchange is carried out through vertical convection, the temperature change of surface seawater can only affect the depth of about 200 m (Borsa et al., 2014; Jones and Marshall, 1993). It is far from enough to affect the basal melting of the Getz Ice Shelf with a thickness of more than 400 m.

In addition, the melting water on the ice shelf surface seeping into the bottom of the ice shelf will also strengthen the basal melting and induce channels (Meierbachtol et al., 2013). However, we found that the number of days that the eastern surface of the Getz Ice Shelf melted from 2003 to 2020 is 0 from the dataset provided by Picard et al. (2007). It means that the influence of Getz's surface meltwater on the change of basal channels can be ignored. Drainage from the bottom of the glacier enters the bottom of the ice shelf through a specific channel, which can enhance the basal melting rate of the ice shelf (Jenkins, 2011; Slater et al., 2015; Le Brocq et al., 2013). The bottom drainage channels of the glacier above the Getz Ice Shelf simulated by some scholars corresponds to some of the basal channels identified in this study (Wei et al., 2020). Due to the lack of drainage monitoring data at the bottom of the glacier, it is difficult to judge the influence of the drainage at the bottom of the glacier on the change of the basal channels.

7 Conclusions

This study first identified and studied the spatial distribution of the basal channels under the Getz Ice Shelf by combining MODIS images, REMA digital elevation models, and IceBridge radar data. We found that basal channels of the Getz Ice Shelf are mainly concentrated in the east of the ice shelf, and most of them are the ocean-sourced basal channel. They mainly came from the concentrated melt at the ice-ocean interface due to the intrusion of warm CDW. From 2009 to 2016, the total length of the basal channels has increased by about 60 km.

Then, we found there is a linear relationship between the shape (cross-sectional area and width) of basal channels and that of the corresponding surface depression. However, this linear relationship did not fit to the hydrostatic equilibrium hypothesis. Therefore, we used this linear relationship instead of the hydrostatic equilibrium hypothesis to develop the long time series of basal channel of the Getz Ice Shelf by combining MODIS images, REMA digital elevation models, IceBridge radar data, ICESat-1 and ICESat-2. The time series allows us to analyze the evolution of basal channels under the Getz Ice Shelf in more detail. The change of the basal channels in the middle and upper reaches of the ice shelf is more significant than that at downstream. It is because that the influence of CDW on basal melting of the Getz Ice Shelf was concentrated where the bottom of the ice shelf is below the 500 m thermocline depth over the troughs. Meanwhile, because of the increase in temperature and the enhancement of intrusion of CDW caused by the changes of wind field surrounding of the Getz Ice Shelf, basal channels have deepened during from 2003–2012 more significantly than that in other periods. In short, our study provides a new idea for future studying and analyzing

the basal melting and its influence on stability of the ice shelf.

Acknowledgements

The wind data are available at https://cds.climate.copernicus.eu/cdsapp#!/dataset/reanalysis-era5-single-levels-monthly-means?tab=form. The CTD data in 2000 and 2007 for this research are from Jacobs et al. (2013) and the CTD data of other years are from MGSD available at https://www.marine-geo.org/tools/new_search/search_map.php?&a=1&data_type=Conductivity&output_info_all=on. The IceBridge data are available at https://nsidc.org/data/IRMCR2/versions/1. The ICESat-1 data are available at https://nsidc.org/data/glah12. The ICESat-2 data are available at https://nsidc.org/data/ATL06/versions/4. The DEM data are available at https://www.pgc.umn.edu/data/rema/.

References

Alley K E, Scambos T A, Siegfried M R, et al. 2016. Impacts of warm water on Antarctic ice shelf stability through basal channel formation. Nature Geoscience, 9(4): 290–293, doi: 10.1038/ngeo2675

Arneborg L, Wåhlin A K, Björk G, et al. 2012. Persistent inflow of warm water onto the central Amundsen shelf. Nature Geoscience, 5(12): 876–880, doi: 10.1038/ngeo1644

Assmann K M, Darelius E, Wåhlin A K, et al. 2019. Warm circumpolar deep water at the western Getz Ice Shelf front, Antarctica. Geophysical Research Letters, 46(2): 870–878, doi: 10.1029/2018GL081354

Bindschadler R, Vaughan D G, Vornberger P. 2011. Variability of basal melt beneath the Pine Island Glacier ice shelf, West Antarctica. Journal of Glaciology, 57(204): 581–595, doi: 10.3189/002214311797409802

Borsa A A, Moholdt G, Fricker H A, et al. 2014. A range correction for ICESat and its potential impact on ice-sheet mass balance studies. The Cryosphere, 8(2): 345–357, doi: 10.5194/tc-8-345-2014

Chartrand A M, Howat I M. 2020. Basal channel evolution on the Getz Ice Shelf, West Antarctica. Journal of Geophysical Research: Earth Surface, 125(9): e2019JF005293, doi: 10.1029/2019JF005293

Cochran J R, Tinto K J, Bell R E. 2020. Detailed bathymetry of the continental shelf beneath the Getz Ice Shelf, West Antarctica. Journal of Geophysical Research: Earth Surface, 125(10): e2019JF005493, doi: 10.1029/2019JF005493

Dee D P, Uppala S M, Simmons A J, et al. 2011. The ERA-Interim reanalysis: configuration and performance of the data assimilation system. Quarterly Journal of the Royal Meteorological Society, 137(656): 553–597, doi: 10.1002/qj.828

Dinniman M S, Klinck J M, Hofmann E E. 2012. Sensitivity of circumpolar deep water transport and ice shelf basal melt along the West Antarctic Peninsula to changes in the winds. Journal of Climate, 25(14): 4799–4816, doi: 10.1175/JCLI-D-11-00307.1

Dotto T S, Garabato A C N, Bacon S, et al. 2019. Wind-driven processes controlling oceanic heat delivery to the Amundsen sea, Antarctica. Journal of Physical Oceanography, 49(11): 2829–2849, doi: 10.1175/JPO-D-19-0064.1

Dow C F, Lee W S, Greenbaum J S, et al. 2018. Basal channels drive active surface hydrology and transverse ice shelf fracture. Science Advances, 4(6): eaao7212, doi: 10.1126/sciadv.aao7212

Dupont T K, Alley R B. 2005. Assessment of the importance of ice-shelf buttressing to ice-sheet flow. Geophysical Research Letters, 32(4): L04503, doi: 10.1029/2004GL022024

Dutrieux P, De Rydt J, Jenkins A, et al. 2014. Strong sensitivity of Pine Island ice-shelf melting to climatic variability. Science, 343(6167): 174–178, doi: 10.1126/science.1244341

Farrell S L, Kurtz N, Connor L N, et al. 2011. A first assessment of IceBridge snow and ice thickness data over Arctic sea ice. IEEE Transactions on Geoscience and Remote Sensing, 50(6): 2098–2111, doi: 10.1109/TGRS.2011.2170843

Fretwell P, Pritchard H D, Vaughan D G, et al. 2013. Bedmap2: improved ice bed, surface and thickness datasets for Antarctica. The Cryosphere, 7(1): 375–393, doi: 10.5194/tc-7-375-2013

Fricker H A, Coleman R, Padman L, et al. 2009. Mapping the grounding zone of the Amery Ice Shelf, East Antarctica using InSAR, MODIS and ICESat. Antarctic Science, 21(5): 515–532, doi: 10.1017/S095410200999023X

Fricker H A, Padman L. 2006. Ice shelf grounding zone structure from ICESat laser altimetry. Geophysical Research Letters, 33(15): L15502, doi: 10.1029/2006gl026907

Fürst J J, Durand G, Gillet-Chaulet F, et al. 2016. The safety band of Antarctic ice shelves. Nature Climate Change, 6(5): 479–482, doi: 10.1038/nclimate2912

Greene C A, Blankenship D D, Gwyther D E, et al. 2017. Wind causes Totten Ice Shelf melt and acceleration. Science Advances, 3(11): e1701681, doi: 10.1126/sciadv.1701681

Holland P R, Jenkins A, Holland D M. 2010. Ice and ocean processes in the Bellingshausen Sea, Antarctica. Journal of Geophysical Research: Oceans, 115(C5): C05020, doi: 10.1029/2008JC005219

Howat I M, Porter C, Smith B E, et al. 2019. The reference elevation model of Antarctica. The Cryosphere, 13(2): 665–674, doi: 10.5194/tc-13-665-2019

Hu Kailong, Liu Qingwang, Pang Yong, et al. 2017. Forest canopy height estimation based on ICESat/GLAS data by airborne LiDAR. Transactions of the Chinese Society of Agricultural Engineering, 33(16): 88–95

Jacobs S, Giulivi C, Dutrieux P, et al. 2013. Getz Ice Shelf melting response to changes in ocean forcing. Journal of Geophysical Research: Oceans, 118(9): 4152–4168, doi: 10.1002/jgrc.20298

Jacobs S S, Helmer H H, Doake C S M, et al. 1992. Melting of ice shelves and the mass balance of Antarctica. Journal of Glaciology, 38(130): 375–387, doi: 10.1017/S0022143000002252

Jacobs S S, Jenkins A, Giulivi C F, et al. 2011. Stronger ocean circulation and increased melting under Pine Island Glacier ice shelf. Nature Geoscience, 4(8): 519–523, doi: 10.1038/ngeo1188

Jenkins A. 1999. The impact of melting ice on ocean waters. Journal of Physical Oceanography, 29(9): 2370–2381, doi: 10.1175/1520-0485(1999)029<2370:TIOMIO>2.0.CO;2

Jenkins A. 2011. Convection-driven melting near the grounding lines of ice shelves and tidewater glaciers. Journal of Physical Oceanography, 41(12): 2279–2294, doi: 10.1175/JPO-D-11-03.1

Jenkins A, Dutrieux P, Jacobs S S, et al. 2010. Observations beneath Pine Island Glacier in West Antarctica and implications for its retreat. Nature Geoscience, 3(7): 468–472, doi: 10.1038/ngeo890

Jenkins A, Jacobs S. 2008. Circulation and melting beneath George VI ice shelf, Antarctica. Journal of Geophysical Research: Oceans, 113(C4): C04013, doi: 10.1029/2007JC004449

Jones H, Marshall J. 1993. Convection with rotation in a neutral ocean: a study of open-ocean deep convection. Journal of Physical Oceanography, 23(6): 1009–1039, doi: 10.1175/1520-0485(1993)023<1009:CWRIAN>2.0.CO;2

Joughin I, Padman L. 2003. Melting and freezing beneath Filchner-Ronne Ice Shelf, Antarctica. Geophysical Research Letters, 30(9): 1477, doi: 10.1029/2003GL016941

Joughin I, Smith B E, Holland D M. 2010. Sensitivity of 21st century sea level to ocean-induced thinning of Pine Island Glacier, Antarctica. Geophysical Research Letters, 37(20): L20502, doi: 10.1029/2010gl044819

Krabill W, Hanna E, Huybrechts P, et al. 2004. Greenland Ice Sheet: increased coastal thinning. Geophysical Research Letters, 31(24): L24402, doi: 10.1029/2004GL021533

Kurtz N T, Farrell S L. 2011. Large-scale surveys of snow depth on Arctic sea ice from operation IceBridge. Geophysical Research Letters, 38(20): L20505, doi: 10.1029/2011GL049216

Kwok R, Kacimi S. 2018. Three years of sea ice freeboard, snow depth, and ice thickness of the Weddell Sea from Operation IceBridge and CryoSat-2. The Cryosphere, 12(48): 2789–2801

Lazeroms W M J, Jenkins A, Gudmundsson G H, et al. 2018. Modelling present-day basal melt rates for Antarctic ice shelves using a parametrization of buoyant meltwater plumes. The Cryosphere, 12(1): 49–70, doi: 10.5194/tc-12-49-2018

Le Brocq A M, Payne A J, Siegert M J, et al. 2009. A subglacial water-

flow model for West Antarctica. Journal of Glacialogy, 55: 879–888, doi: 10.3189/002214309790152564

Le Brocq A M, Ross N, Griggs J A, et al. 2013. Evidence from ice shelves for channelized meltwater flow beneath the Antarctic Ice Sheet. Nature Geoscience, 6(11): 945–948, doi: 10.1038/ngeo1977

Li Teng, Liu Yan, Li Tian, et al. 2018. Antarctic surface ice velocity retrieval from MODIS-based mosaic of Antarctica (MOA). Remote Sensing, 10(7): 1045, doi: 10.3390/rs10071045

Ligtenberg S R M, Helsen M M, van den Broeke M R. 2011. An improved semi-empirical model for the densification of Antarctic firn. The Cryosphere, 5(4): 809–819, doi: 10.5194/tc-5-809-2011

Ligtenberg S R M, Munneke P K, van den Broeke M R. 2014. Present and future variations in Antarctic firn air content. The Cryosphere, 8(5): 1711–1723, doi: 10.5194/tc-8-1711-2014

Liu Zhiwei, Zhu Jianjun, Fu Haiqiang, et al. 2020. Evaluation of the vertical accuracy of open global DEMs over steep terrain regions using ICESat data: a case study over Hunan Province, China. Sensors, 20(17): 4865, doi: 10.3390/s20174865

Meierbachtol T, Harper J, Humphrey N. 2013. Basal drainage system response to increasing surface melt on the Greenland ice sheet. Science, 341(6147): 777–779, doi: 10.1126/science.1235905

Mouginot J, Rignot E, Scheuchl B, et al. 2017. Comprehensive annual ice sheet velocity mapping using landsat-8, sentinel-1, and RADARSAT-2 data. Remote Sensing, 9(4): 364, doi: 10.3390/rs9040364

Noh M J, Howat I M. 2017. The surface extraction from TIN based search-space minimization (SETSM) algorithm. ISPRS Journal of Photogrammetry and Remote Sensing, 129: 55–76, doi: 10.1016/j.isprsjprs.2017.04.019

Padman L, Costa D P, Dinniman M S, et al. 2012. Oceanic controls on the mass balance of Wilkins ice Shelf, Antarctica. Journal of Geophysical Research: Oceans, 117(C1): C01010, doi: 10.1029/2011JC007301

Paolo F S, Fricker H A, Padman L. 2015. Volume loss from Antarctic ice shelves is accelerating. Science, 348(6232): 327–331, doi: 10.1126/science.aaa0940

Payne A J, Holland P R, Shepherd A P, et al. 2007. Numerical modeling of ocean-ice interactions under Pine Island Bay's ice shelf. Journal of Geophysical Research: Oceans, 112(C10): C10019, doi: 10.1029/2006JC003733

Picard G, Fily M, Gallee H. 2007. Surface melting derived from microwave radiometers: a climatic indicator in Antarctica. Annals of Glaciology, 46: 29–34, doi: 10.3189/172756407782871684

Pritchard H D, Ligtenberg S R M, Fricker H A, et al. 2012. Antarctic ice-sheet loss driven by basal melting of ice shelves. Nature, 484(7395): 502–505, doi: 10.1038/nature10968

Rignot E, Jacobs S, Mouginot J, et al. 2013. Ice-shelf melting around Antarctica. Science, 341(6143): 266–270, doi: 10.1126/science.1235798

Rignot E, Steffen K. 2008. Channelized bottom melting and stability of floating ice shelves. Geophysical Research Letters, 35(2): L02503, doi: 10.1029/2007GL031765

Scambos T A, Haran T M, Fahnestock M A, et al. 2007. MODIS-based Mosaic of Antarctica (MOA) data sets: continent-wide surface morphology and snow grain size. Remote Sensing of Environment, 111(2–3): 242–257, doi: 10.1016/j.rse.2006.12.020

Sergienko O V. 2013. Basal channels on ice shelves. Journal of Geophysical Research: Earth Surface, 118(3): 1342–1355, doi: 10.1002/jgrf.20105

Shepherd A, Wingham D, Wallis D, et al. 2010. Recent loss of floating ice and the consequent sea level contribution. Geophysical Research Letters, 37(13): L13503, doi: 10.1029/2010GL042496

Shi Jiuxin. 2018. A review of ice shelf-ocean interaction in Antarctica. Chinese Journal of Polar Research, 30(3): 287–302

Silvano A, Rintoul S R, Herraiz-Borreguero L. 2016. Ocean-ice shelf interaction in east Antarctica. Oceanography, 29(4): 130–143, doi: 10.5670/oceanog.2016.105

Silvano A, Rintoul S R, Peña-Molino B, et al. 2018. Freshening by glacial meltwater enhances melting of ice shelves and reduces formation of Antarctic Bottom Water. Science Advances, 4(4): eaap9467, doi: 10.1126/sciadv.aap9467

Slater D A, Nienow P W, Cowton T R, et al. 2015. Effect of near-terminus subglacial hydrology on tidewater glacier submarine melt rates. Geophysical Research Letters, 42(8): 2861–2868, doi: 10.1002/2014GL062494

Steig E J, Ding Q, Battisti D S, et al. 2012. Tropical forcing of Circumpolar Deep Water inflow and outlet glacier thinning in the Amundsen Sea Embayment, West Antarctica. Annals of Glaciology, 53(60): 19–28, doi: 10.3189/2012AoG60A110

Stewart C, Rignot E, Steffen K, et al. 2004. Basal topography and thinning rates of Petermann Gletscher, northern Greenland, measured by ground-based phase-sensitive radar. Bergen: Bjerknes Centre for Climate Research, 43–47

Thoma M, Jenkins A, Holland D, et al. 2008. Modelling circumpolar deep water intrusions on the Amundsen sea continental shelf, Antarctica. Geophysical Research Letters, 35(18): L18602, doi: 10.1029/2008GL034939

Vaughan D G, Corr H F J, Bindschadler R A, et al. 2012. Subglacial melt channels and fracture in the floating part of Pine Island Glacier, Antarctica. Journal of Geophysical Research: Earth Surface, 117(F3): F03012

Wang Zemin, Song Xiangyu, Zhang Baojun, et al. 2020. Basal channel extraction and variation analysis of Nioghalvfjerdsfjorden ice shelf in Greenland. Remote Sensing, 12(9): 1474, doi: 10.3390/rs12091474

Wei Wei, Blankenship D D, Greenbaum J S, et al. 2020. Getz Ice Shelf melt enhanced by freshwater discharge from beneath the West Antarctic Ice Sheet. The Cryosphere, 14(4): 1399–1408, doi: 10.5194/tc-14-1399-2020